PHYSICAL REVIEW C, VOLUME 61, 051302(R)

Multiple solutions of the self-consistency condition in the Walecka model and the validity of the Brown-Rho scaling law

Zhang Ben-wei, Hou De-fu, and Li Jia-rong
Institute of Particle Physics, Hua-Zhong Normal University, Wuhan 430079, China
(Received 22 November 1999; published 5 April 2000)

We investigate the self-consistency condition (SCC) of mean-field theory in the Walecka model and find that the solutions of the SCC are multiple at high temperature and chemical potential. Using the effective Lagrangian approach, we study medium effects on the ω meson mass by taking into account vacuum effects. We show that the ω meson mass decreases with both temperature and chemical potential with a general tendency, while near the critical point several ω meson masses degenerate due to the multiple solutions of the SCC. We check the validity of the Brown-Rho scaling law in this case. Finally, we calculate the thermodynamic potential and prove that the multiple solutions of the SCC result from a first-order phase transition of nuclear matter in the Walecka model at high temperature and chemical potential.

PACS number(s): 21.65.+f, 14.40.Cs, 11.10.Wx

Investigations of how the properties of hadrons are modified at high temperature and/or density have attracted a lot of attention recently [1–12,16]. These studies can help us to better understand the properties of the chiral phase transition and the quark-gluon plasma, which is expected to be created in relativistic heavy ion collisions. One of the most interesting issues concerns the vector meson masses in media. The dependence of vector meson properties on the temperature and/or the density of the nuclear medium is far from being well understood. There are still a lot of controversies: the results obtained by different methods do not coincide. Some authors [3,4] find the vector meson masses decrease with temperature and/or density which is interpreted as evidence of the partial restoration of chiral symmetry [5,6]. For example, with effective chiral Lagrangians and a suitable incorporation of the scaling property of QCD, it has been shown [1] that the effective masses of σ,ρ,ω mesons and nucleons satisfy the approximate in-medium scaling law

$$\frac{m_\sigma^*}{m_\sigma}\approx\frac{m_\rho^*}{m_\rho}\approx\frac{m_\omega^*}{m_\omega}\approx\frac{m_N^*}{m_N}. \tag{1}$$

In contrast, others [7,8] have proven that the vector meson masses increase in hot and/or dense matter by using effective theories. In addition, because the vacuum structure in hot and/or dense medium is changed, the vacuum effect on the vector meson masses should be taken into account [1,9–12]. Using this idea some authors [10–12] also calculate the vector meson masses by using the effective Langrangian approach and find the vector meson masses are reduced at either finite temperature or density. In order to include the vacuum effect in media, some calculations use the Walecka model to get the effective nucleon mass M^* from the self-consistent condition (SCC) $M^*=M-g_s\phi$ by using mean-field theory (MFT). One obtains a single solution M^* in all regions of the parameter space. In this Rapid Communication, we perform a careful and detailed investigation of these issues and find some new results. We first study the SCC in MFT of the Walecka model and find the solutions of the SCC are multiple for some values of the thermodynamic parameters. Then we investigate the ω meson mass in hot and dense matter within the imagine time formalism of finite temperature field theory. We consider an ωNN interaction and include vacuum effects (see Fig. 1). We show that the ω meson mass decreases with both temperature and chemical potential with an overall tendency, while multiple ω meson masses degenerate at some values of the temperature and the chemical potential. Finally we use our concrete numerical results to check the Brown-Rho scaling law, Eq. (1), at different temperatures and chemical potentials and give a physical interpretation for the multiple solutions in terms of the thermodynamic potential.

We begin by using the Walecka model (often called QHD-I) [13] to get the changes of the nucleon mass at finite temperature and density. The Lagrangian density in the Walecka model is given by

$$\mathcal{L}=\bar{\psi}[\gamma_\mu(i\partial^\mu-g_v V^\mu)-(M-g_s\phi)]\psi+\frac{1}{2}(\partial_\mu\phi\partial^\mu\phi - m_s^2\phi^2)-\frac{1}{4}F_{\mu\nu}F^{\mu\nu}+\frac{1}{2}m_v^2V_\mu V^\mu+\delta\mathcal{L},$$

which contains fields for baryons $p,n(\psi)$, the neutral scalar meson $\sigma(\phi)$, and the vector meson $\omega(V_\mu)$. From MFT [14], the SCC can be derived as

$$M^*=M-g_s\phi=M-\frac{g_s^2}{m_s^2}\frac{2}{\pi^2}\int p^2dp\,\frac{M^*}{\omega_N^*}[n_p(T)+\bar{n}_p(T)], \tag{2}$$

where M^* is the nucleon effective mass and

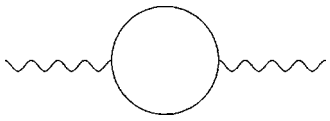

FIG. 1. One-loop diagram for ω meson self-energy in the ωNN interaction.

 ©2000 The American Physical Society

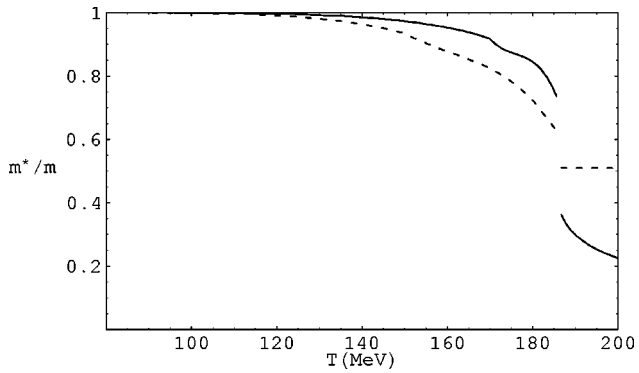

FIG. 2. The temperature dependence of M_N^*/M_N and m_ω^*/m_ω at $\mu=0$ when there is a single solution for M^* and m_ω^*. The solid line represents M_N^*/M_N and the dashed line represents m_ω^*/m_ω. When $T\sim 186$ MeV each line has a cut, which means there are multiple solutions for M^* and m_ω^*.

$$n_p(T)=\frac{1}{e^{\beta(\omega_N^*-\mu)}+1},\quad \overline{n}_p(T)=\frac{1}{e^{\beta(\omega_N^*+\mu)}+1},$$

$$\omega_N^*=\sqrt{p^2+M^{*2}},\quad \beta=\frac{1}{T}.$$

This expression indicates that the main contribution to the reduction of M^* comes from the effect of the scalar σ meson. Taking the parameters [14] $g_s^2=109.626$ and $m_s=520$ MeV, we can get the nucleon effective mass M^* by numerically solving Eq. (2). The results are depicted in Figs. 2–6. We can see that M^* decreases with temperature T and chemical potential μ, and when T and μ are not very large there is only one solution of the SCC. However, as T and μ become larger there appear three different solutions for the nucleon effective mass. In Fig. 2 we show the dependence of M^* on the temperature T when the chemical potential $\mu=0$. There are three solutions for M^* when T ranges from 185.7 to 186.6 MeV. This very narrow range was ignored in the previous literature and consequently all previous calculations obtained a single solution of the SCC for M^*.[1] In Fig. 3 we draw the multiple solutions for M^* in detail in the range and we can easily see the three different solutions for M^* in this range. For example, when $T=185.8$ MeV we get $M^*=390.49$, $M^*=455.813$, or $M^*=683.377$ MeV as the solutions of the SCC. When $T=186.4$ MeV we get $M^*=352.134$, $M^*=534.399$, or $M^*=648.193$ MeV. From Figs. 4 and 5 we find the same phenomenon in the dependence of M^* on T when $\mu=200$ MeV, but the parameter range corresponding to multiple solutions enlarges to nearly 7 MeV. In Fig. 6 we show the μ dependence of M^* when $T=100$ MeV. We find the three solutions appear in a large range of nearly 200 MeV.

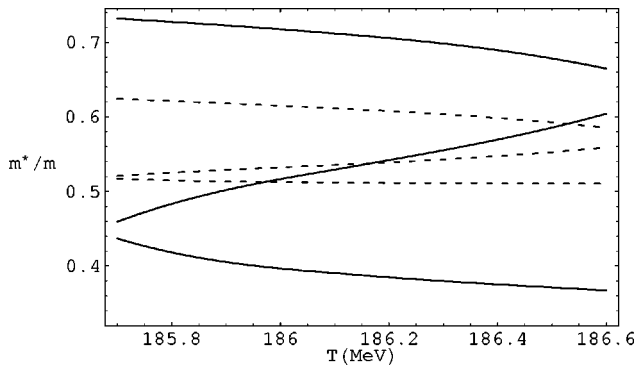

FIG. 3. The temperature dependence of M_N^*/M_N and m_ω^*/m_ω at $\mu=0$ in the range 185.7 to 186.6 MeV where multiple solutions for M^* and m_ω^* exist. The solid line represents M_N^*/M_N and the dashed line represents m_ω^*/m_ω.

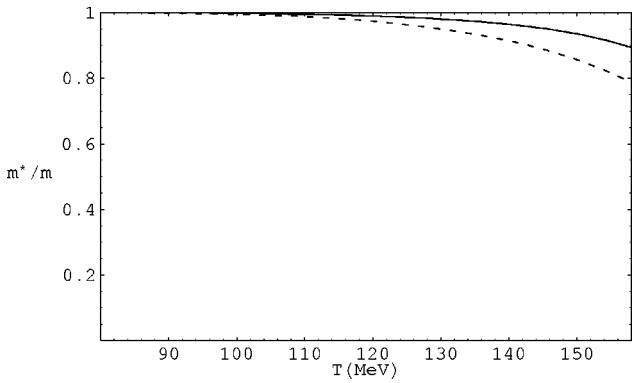

FIG. 4. The temperature dependence of M_N^*/M_N and m_ω^*/m_ω at $\mu=200$ MeV where there is a single solution for M^* and m_ω^*. The solid line represents M_N^*/M_N and the dashed line represents m_ω^*/m_ω.

Next we turn to study the ω meson effective mass in hot and dense matter. In Minkowski space the self-energy can be generally expressed as

$$\Pi^{\mu\nu}=FP_L^{\mu\nu}+GP_T^{\mu\nu}, \tag{3}$$

where $P_L^{\mu\nu}$ and $P_T^{\mu\nu}$ are standard longitudinal and transverse projection tensors, respectively, and are defined as

$$P_T^{00}=P_T^{0i}=P_T^{i0}=0, P_T^{ij}=\delta^{ij}-\frac{k^ik^j}{\mathbf{k}^2}, P_L^{\mu\nu}=\frac{k^\mu k^\nu}{k^2}-g^{\mu\nu}-P_T^{\mu\nu}. \tag{4}$$

The full propagator of the ω meson reads

$$\mathcal{D}^{\mu\nu}=-\frac{P_L^{\mu\nu}}{k^2-m_\omega^2-F}-\frac{P_T^{\mu\nu}}{k^2-m_\omega^2-G}-\frac{k^\mu k^\nu}{m_\omega^2k^2}. \tag{5}$$

By making use of Eqs. (3) and (4), one can show

$$F(k)=\frac{k^2}{\mathbf{k}^2}\Pi^{00}(k),\quad G(k)=-\frac{1}{2}\left[\Pi_i^i+\frac{k_0^2}{\mathbf{k}^2}\Pi^{00}(k)\right]. \tag{6}$$

[1]Serot [14] once speculated that there might be several solutions of SCC for fixed T and μ, but he did not give concrete and affirmative results.

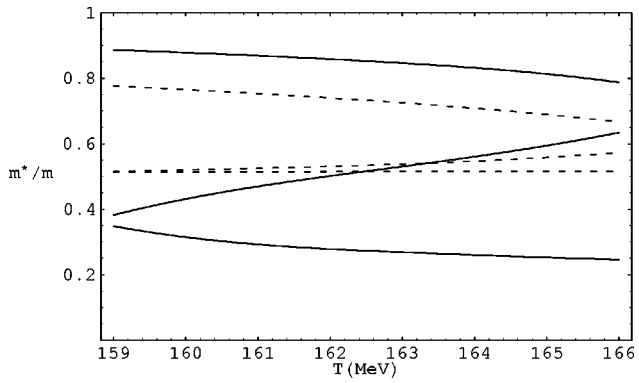

FIG. 5. The temperature dependence of M_N^*/M_N and m_ω^*/m_ω at $\mu=200$ MeV where there appear several solutions for M^* and m_ω^* and T ranges from 159 to 166 MeV. The solid line represents M_N^*/M_N and the dashed line represents m_ω^*/m_ω.

In order to get the effective mass of the ω meson, we take the limit $\mathbf{k}\to 0$, and show that $F=G$ and $k^2=k^{0^2}-\mathbf{k}^2=\omega^2$. The effective mass of the ω meson in a hot and dense medium is obtained from the pole of the full propagator

$$\omega^2-m_\omega^2-\mathrm{Re}[\lim_{\mathbf{k}\to 0}F(k)]=0. \tag{7}$$

The Lagrangian density for ωNN interaction reads

$$\mathcal{L}_I=g_{\omega NN}\bar{\psi}\gamma_\mu\omega^\mu\psi, \tag{8}$$

where ω^μ and ψ are the ω meson and nuclear fields, respectively. Using the imaginary-time formalism of the finite temperature field theory, one can obtain the self-energy for the ω meson (Fig. 1)

$$\Pi_\rho^{\mu\nu}=2g_{\rho NN}^2T\sum_{n=-\infty}^{+\infty}\int\frac{d^3p}{2\pi^3}\mathrm{Tr}\left[\gamma_\mu(k)\frac{1}{\gamma^s p_s-M^*}\times\gamma_\nu(-k)\frac{1}{\gamma^s(p_s-k_s)-M^*}\right], \tag{9}$$

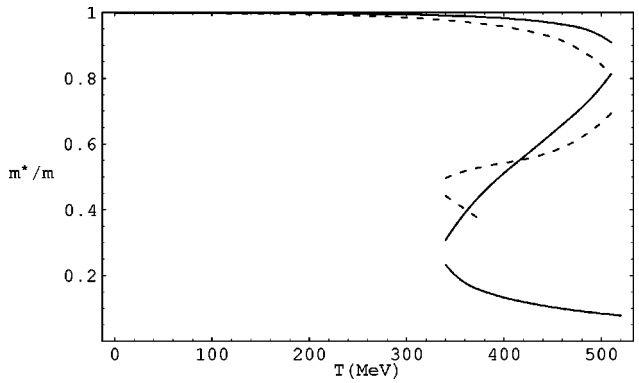

FIG. 6. The chemical potential dependence of M_N^*/M_N and m_ω^*/m_ω at $T=100$ MeV. The solid line represents M_N^*/M_N and the dashed line represents m_ω^*/m_ω.

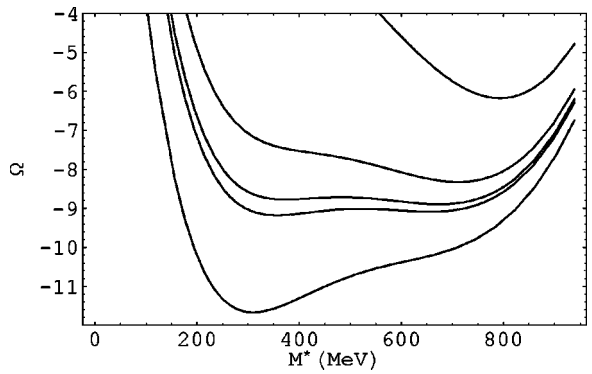

FIG. 7. The isotherms of the thermodynamic potential as a function of M^* at $\mu=0$. From top to bottom the five lines represent the isotherms of the thermodynamic potential at $T=180$, 185, 186, 186.3, and 188 MeV, respectively.

with $p_0=(2n+1)\pi Ti+\mu$, $k_0=2l\pi Ti$. By making use of the mathematical expression

$$T\sum f(p_0=(2n+1)\pi Ti+\mu)=\frac{T}{2\pi i}\oint dp_0 f(p_0)\frac{1}{2}\beta\tanh\left[\frac{1}{2}\beta(p_0-\mu)\right],$$

one can separate the vacuum contributions from the matter contributions [15]:

$$\begin{aligned}T\sum f(p_0=(2n+1)\pi Ti+\mu)&=-\frac{1}{2\pi i}\int_{-i\infty+\mu+\epsilon}^{+i\infty+\mu+\epsilon}dp_0 f(p_0)\frac{1}{e^{\beta(p_0-\mu)}+1}\\&\quad-\frac{1}{2\pi i}\int_{-i\infty+\mu-\epsilon}^{+i\infty+\mu-\epsilon}dp_0 f(p_0)\frac{1}{e^{-\beta(p_0-\mu)}+1}\\&\quad+\frac{1}{2\pi i}\int_{-i\infty}^{+i\infty}dp_0 f(p_0-\mu).\end{aligned}$$

The first two terms correspond to matter contributions as functions of temperature and chemical potential, while the last term accounts for vacuum contributions.

The last term is divergent. Using dimensional regularization to get rid of the divergence, we obtain from Eq. (7)

$$\Pi_{vac}^{\mu\nu}(k)=\frac{g_{\omega NN}^2}{\pi^2}(k^\mu k^\nu-k^2g^{\mu\nu})\omega^2\int_0^1 dzz(1-z)\ln\left[\frac{M^{*2}-\omega^2z(1-z)}{M^2-m_\omega^2z(1-z)}\right]. \tag{10}$$

Using the residue theorem and the periodicity condition of k_0 in the finite temperature field theory [15], we can then get the matter contribution,

$$\Pi^{00}_{mat}(k) = -\frac{g^2_{\omega NN}}{\pi^2}\int dp\,\frac{p^2}{\omega^*_N}[n_p(T)+\overline{n}_p(T)] \times\left[2+\frac{4\omega^*_N k^0-4\omega^{*2}_N-k^2}{4p|\mathbf{k}|}\ln\frac{k^2-2k^0\omega^*_N+2p|\mathbf{k}|}{k^2-2k^0\omega^*_N-2p|\mathbf{k}|} + \frac{-4\omega^*_N k^0-4\omega^{*2}_N-k^2}{4p|\mathbf{k}|}\ln\frac{k^2+2k^0\omega^*_N+2p|\mathbf{k}|}{k^2+2k^0\omega^*_N-2p|\mathbf{k}|}\right],$$

$$(\Pi^i_i(k))_{mat} = -2\frac{g^2_{\omega NN}}{\pi^2}\int dp\,\frac{p^2}{\omega^*_N}[n_p(T)+\overline{n}_p(T)] \times\left[2-\frac{2M^*+k^2}{4p|\mathbf{k}|}\left(\ln\frac{k^2-2k^0\omega^*_N+2p|\mathbf{k}|}{k^2-2k^0\omega^*_N-2p|\mathbf{k}|} + \ln\frac{k^2+2k^0\omega^*_N+2p|\mathbf{k}|}{k^2+2k^0\omega^*_N-2p|\mathbf{k}|}\right)\right],$$

where $\omega^*_N > \mu$. From Eq. (7) we can obtain $F(k)$ and $G(k)$ which allow us to study the dependence of m_ω on the momentum $\mathbf{k}$. However, we are interested here in the effective mass of the ω meson, thus we take the limit $\mathbf{k}\to 0$ and find

$$\mathrm{Re}[\lim_{\mathbf{k}\to 0}F_{vac}(k)] = \frac{g^2_{\rho NN}}{\pi^2}\omega^2\int_0^1 dz z(1-z)\ln\left[\frac{M^{*2}-\omega^2 z(1-z)}{M^2-m^2_\omega z(1-z)}\right], \quad (11)$$

$$\mathrm{Re}[\lim_{\mathbf{k}\to 0}F_{mat}(k)] = -\frac{4g^2_{\rho NN}}{\pi^2}\int p^2 dp\,\frac{1}{\omega^*_N(\omega^2-4\omega^{*2}_N)} \times\left[\frac{1}{e^{\beta(\omega^*_N+\mu)}+1}+\frac{1}{e^{\beta(\omega^*_N-\mu)}+1}\right]\left(\frac{4}{3}p^2+2M^{*2}\right). \quad (12)$$

Note that the ωNN interaction will affect M^*. However, as has been pointed out by other authors [16], the effects due to vector meson exchange upon M^* are very small and can be neglected. This procedure is consistent with our treatment of the nucleon mass M^* since M^* is determined only by the scalar and fermion fields within the Walecka model in MFT, and there will be no effect on M^* from vector mesons.

With M^* given by Eq. (2) we can solve Eq. (7) numerically and determine the modified meson mass m^*_ω as a function of temperature and chemical potential. We choose a coupling of $g^2_{\omega NN}/4\pi = 20.0$ [17]. In Figs. 2–5 we show the temperature dependences of the ω meson mass at $\mu = 0$ and $\mu = 200$ MeV, respectively, and find that the ω meson mass decreases with temperature with an overall tendency. Figure 6 shows the chemical potential dependence of the ω meson mass at $T = 100$ MeV. The ω meson mass also decreases with increasing chemical potential μ with a general tendency, which is consistent with the results of other authors [18]. However, in contrast to the results of other authors we find that for high T and/or μ there may be several solutions for ω meson masses. Using our results we can check the Brown-Rho scaling law (1). We draw the curves of the T and μ dependences of M^*_N/M_N and m^*_ω/m_ω in Figs. 2–6. We find that the scaling law works well when T and μ are not too high and there is a single solution for M^* and m^*_ω. But when the temperature and chemical potential are large, the scaling law will be broken, since there are several different solutions for M^* and m^*_ω.

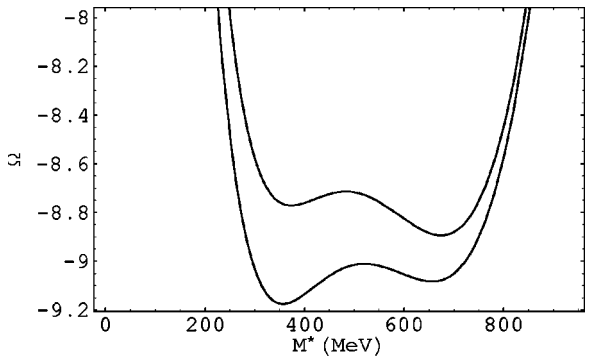

FIG. 8. An enlargement of the isotherms of the thermodynamic potential Ω at $\mu = 0$ when Ω has three extreme points at $T \sim 186$ MeV.

In order to get deeper insight into the multiple solutions of the SCC, we calculate the thermodynamic potential for the Walecka model [19],

$$\Omega = \frac{1}{2}(m^2_s\phi^2 + m^2_v\mathbf{V}^2 - m^2_v V^2_0)V - T\sum_{\mathbf{p},\lambda}[\ln(1+e^{-\beta(\omega^*_N-\mu)}) + \ln(1+e^{-\beta(\omega^*_N+\mu)})].$$

In this expression, the sums run over all single-particle states labeled by momenta $\mathbf{p}$ and intrinsic quantum number λ. From the thermodynamic potential one can obtain all of the thermodynamic functions. As shown in Fig. 7, from the isotherms of the thermodynamic potential as a function of M^*, we find that when T is not too high, the thermodynamic potential only has one extreme point, but as T increases to

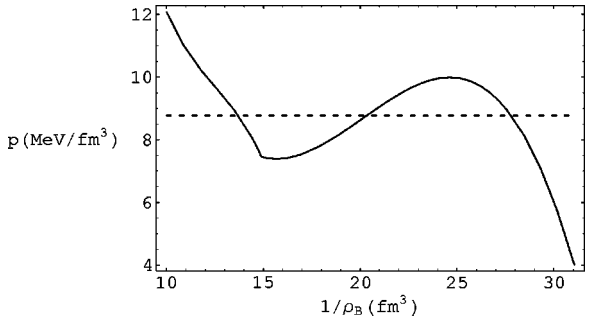

FIG. 9. The phase diagram in nuclear matter: pressure as a function of proper volume/baryon for $T = 100$ MeV. The dashed line is Maxwell isotherm.

near 186 MeV, there are three extreme points, which correspond with the three solutions for M^*. Furthermore, when T continues to increase, there is again only one extreme point. The amplified region where the thermodynamic potential has three extreme points is depicted more clearly in Fig. 8. In Fig. 9 we show the phase diagram of nuclear matter in the Walecka model. This diagram looks quite similar to the Van Der Waals isotherm of gas-liquid transitions. Figures 7–9 indicate explicitly that nuclear matter described by the Walecka model has a first-order phase transition at high temperature and density, which results in multiple solutions for the nucleon and ω meson masses.

In summary, we have studied the nucleon effective mass within the Walecka model in the imagine time formalism of finite temperature field theory. Within the effective Lagrangian approach we investigate the medium effects on the ω meson mass and include the vacuum effects. We show that m_ω^* decreases with both temperature and chemical potential with an overall tendency. From the thermodynamic potential and the phase diagram we find that the Walecka model in MFT predicts a first-order phase transition at high temperature and chemical potential, which consequently leads to multiple solutions for M^* and m_ω^*, and which results in the breaking of the Brown-Rho scaling law. Of course our results may depend on the model and might only occur within the mean-field approximation. It would be interesting to extend this work to other models and to go beyond MFT. In this Rapid Communication, we have only discussed the ω meson effective mass in media, but our discussions can also be applied to the ρ meson mass in hot and/or dense matter, and we expect similar results will be obtained.

We are grateful to M. E. Carrington for a careful reading of the manuscript. This work was supported in part by the National Natural Science Foundation of China (NSFC) under Grant No. 19775017.

[1] G. E. Brown and M. Rho, Phys. Rev. Lett. **66**, 2720 (1991).
[2] V. L. Eletsky and B. L. Ioffe, Phys. Rev. Lett. **78**, 1010 (1997).
[3] T. Hatsuda and S. H. Lee, Phys. Rev. C **46**, 34 (1992).
[4] M. Asakawa and C. M. Ko, Nucl. Phys. **A572**, 732 (1994).
[5] G. E. Brown *et al.*, Phys. Rev. Lett. **60**, 2723 (1988).
[6] K. Kubodera and M. Rho, Phys. Rev. Lett. **67**, 3479 (1991).
[7] C. Gale and J. I. Kapusta, Nucl. Phys. **B357**, 65 (1991).
[8] A. Hosaka, Phys. Lett. B **244**, 363 (1990).
[9] A. Mishra *et al.*, Phys. Rev. C **56**, 1380 (1997).
[10] Chungsik Song *et al.*, Phys. Rev. C **52**, 408 (1995).
[11] H. C. Jean *et al.*, Phys. Rev. C **49**, 1981 (1994).
[12] H. Shiomo and T. Hatsuda, Phys. Lett. B **334**, 281 (1994).
[13] J. D. Walecka, Ann. Phys. (N.Y.) **83**, 491 (1974).
[14] B. D. Serot, Rep. Prog. Phys. **55**, 1855 (1992).
[15] J.I. Kapusta, *Finite Temperature Field Theory* (Cambridge University Press, Cambridge, 1989).
[16] Y. J. Zhang *et al.*, Phys. Rev. C **56**, 3336 (1997); Ping Wang *et al.*, *ibid.* **59**, 928 (1999).
[17] R. Machleidt *et al.*, Phys. Rep. **149**, 1 (1987).
[18] P. Maris *et al.*, Phys. Rev. C **57**, 2821 (1998).
[19] R. J. Furnstahl and B. D. Serot *et al.*, Phys. Rev. C **43**, 105 (1991).